Putative disease gene identification and drug repurposing for Charcot-Marie-Tooth disease

Pietro Sciabbarrasi & Santiago Vessi

GROUP 02
June 2025

Abstract

Charcot-Marie-Tooth disease was studied using a network-based bioinformatics approach integrating DIAMOnD, DiaBLE, and Heat-diffusion to predict novel genes via the human interactome. Enrichment analysis on 100 predicted genes revealed functional overlaps with known CMT genes. Top 20 genes were queried in DGIdb for drug repurposing, with the top three drugs cross-checked in clinicaltrials.gov for ongoing CMT trials.

1 Introduction

Charcot-Marie-Tooth (CMT) disease is a group of inherited neuropathies affecting the peripheral nervous system, characterized by progressive muscle weakness and sensory loss [1]. Despite advances in identifying causative genes, many remain undiscovered. This study employs network-based approaches to identify potential CMT-associated genes by analyzing the human interactome. We applied three algorithms : DIAMOnD, DiaBLE, and Heat Diffusion, to prioritize new candidate genes related to CMT. By leveraging known CMT-associated genes as seeds and integrating interactomic data, our goal is to enhance gene discovery and guide drug repurposing strategies. We further validate the best predictions through enrichment analysis and explore their therapeutic potential using drug-gene interaction databases.

2 Materials and Methods

2.1 PPI and GDA data gathering and interactome reconstruction

To reconstruct a reliable and biologically meaningful human interactome, we collect protein–protein interaction (PPI) data from the BioGRID database, which aggregates experimentally validated interactions from multiple high-quality studies. We consider only physical interactions between human proteins, removing self-interactions and interactions involving non-coding elements. Concurrently, we extract known gene–disease associations (GDAs) for Charcot-Marie-Tooth disease from diseases.jensenlab.org. We validate and standardize these gene symbols using the HUGO Gene Nomenclature Committee (HGNC) tool to ensure consistency and correct mapping to the interactome.
From the human interactome, we extract a subgraph containing only the nodes corresponding to the CMT-associated genes. Since this subgraph is not fully connected, we isolate its Largest Connected Component (LCC) to ensure that all nodes are mutually reachable for algorithms that rely on network topology. The resulting LCC serves as the disease-specific network used as input for gene prioritization.

2.2 Comparative analysis of the disease genes identification algorithms

We evaluate three algorithms for disease gene prediction: DIAMOnD, DiaBLE, and Heat Diffusion, each applied to the same set of known CMT genes mapped onto the Largest Connected Component of the human interactome.
DIAMOnD (Disease Module Detection) iteratively expands the disease module by selecting, at each step, the node most significantly connected to the current module, based on a hypergeometric test of node connectivity. In contrast, DiaBLE (Disease gene prioritization using Link-Based Enrichment) implements a statistical framework that evaluates the significance of observed links between seed genes and candidate genes across the interactome, producing both scores and p-values for each gene. Finally, the Heat Diffusion algorithm models the propagation of information from

seed genes across the network structure by simulating a diffusion process, ranking genes based on their steady-state heat scores, which reflect topological proximity to the input seeds.
To assess the robustness and predictive power of the three algorithms, we implement a 5-fold cross-validation strategy using the curated set CMT-associated genes within the Largest Connected Component (LCC) of the human interactome. The gene set is randomly partitioned into five disjoint subsets. At each fold, four subsets serve as the training set (seed genes), while the remaining subset is held out as the test set. Each algorithm is then executed using only the training genes, generating a ranked list of candidate genes based on network topology and algorithm-specific scoring criteria.
To evaluate prediction performance, we compute precision, recall, and F1-score at multiple top-k thresholds (top $\frac{1}{4}n$, $\frac{1}{2}n$, 50, n) where n is the number of known GDAs or seed genes, focusing on the recovery of test genes from the ranked lists. To ensure that the ranking reflects the model's ability to generalize beyond known associations all seed genes used during training are explicitly removed from the prediction outputs prior to evaluation.

2.3 Putative disease gene identification

Following the comparative evaluation of the three algorithms, we select the one with the best overall performance in terms of precision, recall, and F1-score. Using this method, we generate a list of 200 putative disease genes not previously associated with Charcot-Marie-Tooth disease. From this list, the top 100 genes are retained for downstream functional validation.
To assess their potential biological relevance, we perform functional enrichment analysis using the EnrichR library, using sources from: Gene Ontology—Biological Process (GO-BP), Molecular Function (GO-MF), and Cellular Component (GO-CC)—as well as Reactome and KEGG pathways. The same enrichment analysis is also applied to the original set of known CMT-associated genes to establish a functional baseline. Finally, we compare the enriched terms between the original and the putative gene sets to identify overlaps in biological processes, molecular functions, or pathways that may support the relevance of the predictions.

2.4 Drug repurposing

To explore the therapeutic potential of the predicted disease-associated genes, we perform a drug repurposing analysis in two main steps: drug identification and clinical trials validation.
We select the top 20 putative disease genes from the ranking obtained using the best-performing gene prioritization algorithm. These genes are cross-referenced against the latest version of the Drug–Gene Interaction Database DGIdb.org using the `interactions.tsv` file retaining only FDA-approved compounds. Drugs are ranked based on the number of distinct predicted genes they target, with priority given to those interacting with the highest number of top-ranked genes.
Subsequently, we take the top three drugs from this ranking and manually verify their clinical relevance by querying clinicaltrials.gov. The number of retrieved clinical trials is noted for each compound, and representative trials are optionally recorded by reporting their title and identifier.
This pipeline identifies approved drugs linked to the predicted gene set, though the absence of specific trials in our case highlights the early-stage of these findings and the need for further validation in future studies.

2.5 Work Execution

For our work, we used `Python` as the programming language. The libraries employed were `NetworkX`, `Pandas`, `NumPy`, `Matplotlib`, `Scikit-learn`, `SciPy`, and `Seaborn`, primarily for data extraction and graph analysis. Additionally, `GSEApy` was used for enrichment analysis. The DIAMOnD algorithm was implemented using code from GitHub user `dinaghiassian`, while custom scripts were developed for DiaBLE and Heat Diffusion.

3 Results and Discussion

3.1 PPI and GDA data gathering and interactome reconstruction

The human interactome constructed, resulted in a network with 20,045 nodes and 871,700 edges. The largest connected component included the entire graph, indicating that no node, each representing a gene, was isolated, and that a path existed between every pair of nodes in the network.
In Table 1, we observe that, of the initial 87 known gene-disease associations for Charcot-Marie-Tooth disease, nine genes were not present in the analyzed network. The resulting disease-specific interactome contains 79 nodes and 101 edges. Its largest connected component includes 57 nodes and 100 edges, revealing that more than 20 nodes were isolated in the original graph.

Disease name	UMLS disease id	MeSH disease class	Number of associated genes	Number of genes present in the interactome	LCC size of the disease interactome
Charcot-Marie-Tooth Disease	C0007959	C10	87	79	57

Table 1: Summary of GDAs and basic network data

As shown in Table 6, *VCP* exhibits the highest degree (15), establishing it as a central hub with extensive connections. *RAB7A* (13) and *BAG3* (10) also have high degrees, suggesting significant roles in the network. In contrast, several genes, such as *FIG4*, *PLEKHG5*, and *PDK3*, have a degree of 1, indicating minimal connectivity and likely peripheral roles.

VCP also has the highest betweenness centrality (0.314644), reinforcing its critical role in connecting different parts of the network. *RAB7A* (0.239473) and *LMNA* (0.189731) similarly exhibit high betweenness, indicating their roles as key intermediaries. Twenty-one genes, including PMP22 and MFN2, which are among the most frequently mutated in CMT [2], exhibit zero betweenness centrality, indicating they do not act as bridges in the CMT interactome.

In terms of eigenvector centrality, *VCP* (0.405163), *RAB7A* (0.364040), and *BAG3* (0.303257) score highly, indicating connections to other influential genes. Despite the network's small size, closeness centrality ranges from 0.20 to 0.50 with low variance, with *VCP*, *RAB7A*, and *INF2* having the highest values. These genes, along with *BAG3*, consistently rank high across multiple metrics, underscoring their central, influential, and well-positioned roles in the network, as further illustrated in Figure 1.

The betweenness-to-degree ratio highlights *NEFL* (0.023360) as having a critical bridging role despite a low degree (4), suggesting its importance in linking network components. *LMNA* (0.021081) and *VCP* (0.020976) also have high ratios, reinforcing their roles as key connectors in the CMT interactome.

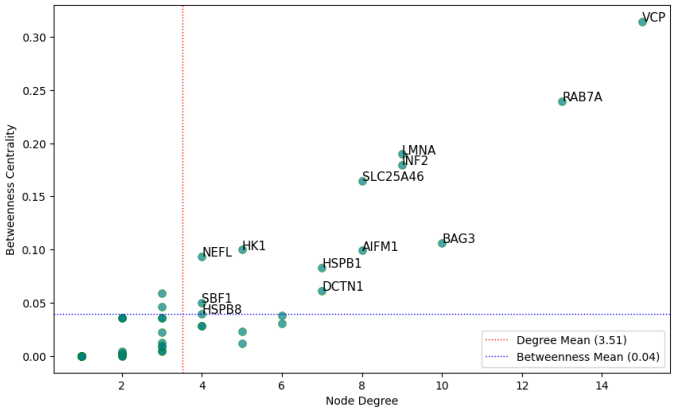

Figure 1: node degree vs node betweenness in the disease LCC

3.2 Comparative analysis of the disease genes identification algorithms

The DIAMOnD, DiaBLE, and Heat Diffusion algorithms produced distinct sets of putative genes associated with Charcot-Marie-Tooth disease (Table 2). Using default parameters for the DIAMOnD and DiaBLE algorithms, we identified 163 unique genes out of the 200 genes outputted. For the Heat Diffusion algorithm, results remained consistent across all three diffusion times applied (t = 0.002, 0.005, 0.01). The DIAMOnD algorithm produced the highest number of unique genes, while the other algorithms returned significantly fewer unique results. Only eleven genes were common across all methods: *FIS1*, *EXD2*, *ALDH3A2*, *RHOT2*, *RAB3B*, *MARCH5*, *MTCH1*, *FKBP8*, *OCIAD1*, *VPS13D*, and *TDRKH*.

Total genes in DIAMOnD output	200	**Number of genes common in DIAMoND and Heat:**	23	**Number of genes unique to DIAMOnD**	151
Total genes in DiaBLE output	200	**Number of genes common in DiaBLE and DIAMOnD**	37	**Number of genes unique to DiaBLE**	155
Total genes in Heat output	200	**Number of genes common in Heat and DiaBLE:**	19	**Number of genes unique to Heat**	169

Table 2: Summary of Algorithms

We then performed a 5-fold cross-validation (Table 3). Due to the non-deterministic nature of the computations and generally low values across all performance metrics (Precision, Recall, F1 Score), we could not definitively determine which method was superior. However, the DIAMOnD algorithm appeared to perform slightly better in most cases (Figures 2,3, and 4).

At the cut-off of 14, DIAMOnD had the highest mean scores across all metrics, though the standard deviations were significant, suggesting variability in performance across folds. The DiaBLE algorithm followed, with slightly lower values in all the metrics, while Heat Diffusion failed to produce any correct predictions (Precision, Recall, and F1 Score all equal to 0), indicating limitations of this method at such a stringent cut-off. As we relaxed the cut-off, DIAMOnD consistently maintained higher Precision and Recall compared to DiaBLE and Heat Diffusion, though the differences narrowed.

Notably, Heat Diffusion showed an improvement at cut-off 57 (Precision = 0.017 ± 0.0, Recall = 0.087 ± 0.003, F1 Score = 0.029 ± 0.0), but the standard deviation of Recall was remarkably low, indicating more consistent performance across folds. However, the absolute values remained low, highlighting the difficulty of gene prediction in Charcot-Marie-Tooth using these methods potentially given by the complexity of disease's genetic architecture.

Cut-off	Method	Precision	Recall	F1 Score
14	DIAMOnD	0.042 ± 0.034	0.051 ± 0.042	0.046 ± 0.038
	DiaBLE	0.028 ± 0.034	0.033 ± 0.041	0.031 ± 0.037
	Heat Diffusion	0.0 ± 0.0	0.0 ± 0.0	0.0 ± 0.0
28	DIAMOnD	0.021 ± 0.017	0.051 ± 0.042	0.03 ± 0.025
	DiaBLE	0.014 ± 0.017	0.033 ± 0.041	0.02 ± 0.024
	Heat Diffusion	0.014 ± 0.017	0.034 ± 0.043	0.02 ± 0.024
50	DIAMOnD	0.016 ± 0.014	0.068 ± 0.062	0.026 ± 0.024
	DiaBLE	0.012 ± 0.016	0.05 ± 0.066	0.019 ± 0.025
	Heat Diffusion	0.012 ± 0.009	0.053 ± 0.043	0.019 ± 0.015
57	DIAMOnD	0.014 ± 0.013	0.068 ± 0.062	0.023 ± 0.021
	DiaBLE	0.014 ± 0.02	0.066 ± 0.097	0.023 ± 0.033
	Heat Diffusion	0.017 ± 0.0	0.087 ± 0.003	0.029 ± 0.0

Table 3: 5-fold cross validation results

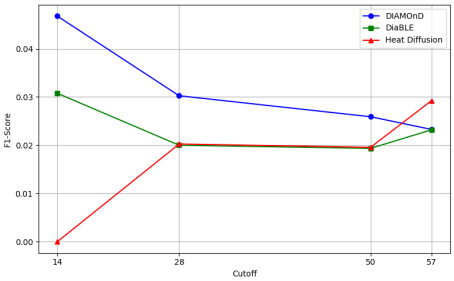

Figure 2: F1-Score

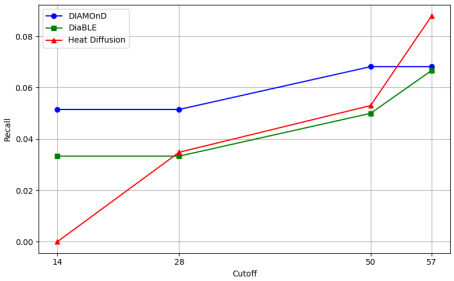

Figure 3: Recall

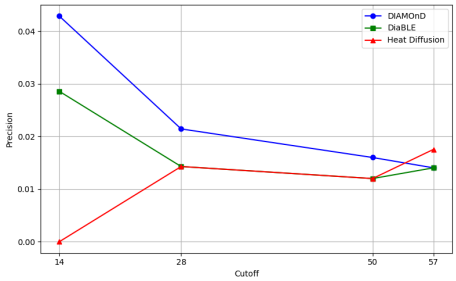

Figure 4: Precision

3.3 Putative disease gene identification

As previously mentioned, DIAMOnD was selected as the most robust method based on its slightly superior overall performance in the cross-validation metrics. Using this algorithm, we generated a ranked list of 200 candidate genes potentially associated with Charcot-Marie-Tooth disease. The top 100 genes of this list were retained for downstream analysis.

To assess the biological plausibility of these predictions, we performed functional enrichment analysis across five knowledge bases: Gene Ontology—Biological Process, Molecular Function, Cellular Component, Reactome and KEGG pathways. We then compared the significantly enriched terms (adjusted p-value ≤ 0.05) between the known and putative gene sets to identify overlapping biological signatures (Table 4).

In GO-BP, we found 87 enriched terms among the putative genes, with 4 terms overlapping with the original set. Notably, shared terms included "mitochondrion organization", "protein targeting to mitochondrion", and "response to unfolded protein", all of which are processes consistent with the mitochondrial dysfunction often implicated in

CMT pathophysiology. Mitochondrial dynamics and transport are known to be essential for axonal maintenance and peripheral nerve function, and defects in mitochondrial organization have been previously linked to demyelinating and axonal forms of CMT [3].
Similarly, in GO-MF, 1 overlapping term was identified ("nucleoside-triphosphatase activity"), which may reflect dysregulation of GTPase relevant to vesicular trafficking and membrane remodeling, also implicated in Schwann cell and axonal function [4]. GO-CC analysis revealed 2 shared components, including "endoplasmic reticulum membrane" and "lipid droplet", both organelles involved in protein folding, calcium signaling, and lipid homeostasis. These functions are recognized in peripheral neuropathies and neurodegeneration [5].
Reactome pathway analysis revealed 4 overlapping terms, particularly those related to Rho GTPase signaling and selective autophagy, both of which play roles in neuronal survival and cytoskeletal regulation, Rho GTPase activity has been associated with axon guidance, Schwann cell migration, and myelin sheath integrity, while autophagy is essential for neuronal maintenance and has been linked to inherited neuropathies, including CMT subtypes associated with impaired protein quality control [6].
KEGG analysis highlighted 2 shared pathways, including "Amyotrophic Lateral Sclerosis (ALS)" and "Pathways of Neurodegeneration", reinforcing the potential neurological relevance of the predicted genes. Although ALS and CMT are distinct disorders, they share several common mechanisms, such as axonal degeneration, impaired axonal transport, and mitochondrial dysfunction. The enrichment of neurodegeneration-related pathways suggests that some of the predicted genes may be involved in broader processes underlying neuronal degeneration, supporting their relevance to our case-study disease [7].
Overall, the convergence of enriched biological terms between known and predicted genes provides evidence supporting the validity of the DIAMOnD-based predictions. These results suggest that the top-ranked putative genes may participate in similar molecular mechanisms as known CMT-associated genes, and so represent promising candidates for further experimental validation.

Biological Process 2021
- establishment of protein localization to mitochondrion - mitochondrion organization - protein targeting to mitochondrion - response to unfolded protein
GO Molecular Function 2021
- nucleoside-triphosphatase activity
GO Cellular Component 2021
- endoplasmic reticulum membrane - lipid droplet
Reactome 2022
- rho gtpase cycle r-hsa-9012999 - selective autophagy r-hsa-9663891 - signaling by rho gtpases r-hsa-194315 - signaling by rho gtpases, miro gtpases and rhobtb3 r-hsa-9716542
KEGG 2021 Human
- amyotrophic lateral sclerosis - pathways of neurodegeneration

Table 4: Overlapping Terms

3.4 Drug repurposing

From the putative genes identified through DIAMonD, we filtered out those not associated with pathways common to both known and putative genes, retaining the top 20 candidates. To refine our analysis, we cross-referenced these genes using the latest Drug-Gene Interaction Database. After reviewing the results (Table 5), we observed that many of the drugs showed no known association with Charcot-Marie Tooth disease. However, three drugs emerged with potential relevance: disulfiram, insulin, and a subset of statins.
Disulfiram, used for treating alcoholism, which works with the gene *ALDH3A2*, could be a good option because it can block the proteasome, the system that breaks down proteins in cells. This is important because in CMT4J, a type of CMT, the *FIG4* protein gets broken down too fast. This causes problems in the cell. A study by Lenk et al. [8] showed that blocking the proteasome helps keep the *FIG4* protein stable and working. This means controlling how proteins are broken down might be a good way to treat CMT. So this drug might help in CMT4J and similar forms of CMT by stopping the breakdown of important proteins, fixing the problem of too much protein loss.
Insulin, known to treat diabetes, was identified via its interaction with *PTPN1*, which slows down insulin signaling,

and this connection is linked to CMT. A study by Oh et al.[9] showed that insulin helps Schwann cells (which make myelin) grow and create more myelin, both in lab tests and in a mouse model of CMT1A. This works through the ERK1/2 and AKT pathways, which are important for cell growth and repair. The treated rodents had faster nerve signals, thicker myelin, and better movement. This may suggest that insulin helps to keep nerves healthy and could be used as a treatment for CMT.

Statins, like simvastatin, have been linked to nerve problems, which is a concern for people with Charcot-Marie-Tooth disease. Statins lower cholesterol but this could possibly harm nerve cells because cholesterol is important for nerve membranes and energy. They can also reduce coenzyme Q10, which is needed for nerve energy production, possibly causing nerve damage. A study on long-term statin use[10] found that it reduced nerve signal strength, especially in nerves that are often affected in CMT. These effects could potentially be more serious for people who already have nerve problems like CMT. This suggests that simvastatin and other statins might make nerve damage worse in CMT, so doctors should be careful when prescribing them for these patients.

In summary, this study identified three drugs—disulfiram, insulin, and statins—as having potential relevance to Charcot-Marie-Tooth disease. Disulfiram may help stabilize important proteins, while insulin could support nerve repair and myelination. However, statins may pose risks to nerve health in CMT patients. A search of clinicaltrials.gov did not reveal any ongoing or completed trials investigating these drugs for CMT, highlighting the preliminary nature of these findings. Nonetheless, the known biological effects of disulfiram and insulin suggest they could be promising candidates for future research.

Drug Name	**Target Gene**
CAPECITABINE	VPS13D
DEHYDRATED ALCOHOL	CAV1
DISULFIRAM	ALDH3A2
INSULIN, REGULAR, HUMAN	PTPN1
PRAVASTATIN SODIUM	RHOA
QUINIDINE	RHOA
SIMVASTATIN	RHOA
TESTOSTERONE	CAV1
TILUDRONIC ACID	PTPN1
VINCRISTINE	STIM1

Table 5: Identified Drugs

4 Conclusions

This study utilized a network-based bioinformatics approach, integrating DIAMOnD, DiaBLE, and Heat Diffusion algorithms, to predict novel genes associated with Charcot-Marie-Tooth disease within the human interactome. Functional enrichment analysis of 100 putative genes identified by the best-performing method revealed significant overlaps with known CMT genes in biological processes, molecular functions, and pathways, supporting the biological relevance of the predictions. In our drug repurposing analysis, we identified disulfiram and insulin as potential candidates for CMT treatment. Conversely, statins were highlighted as potentially harmful for CMT patients due to their known neurotoxic effects.

Several limitations should be acknowledged. The relatively small size of the CMT-specific interactome (57 nodes in the largest connected component) and the low cross-validation performance scores suggest that network-based approaches may be inherently constrained by the current understanding of CMT genetics and protein interactions.

In conclusion, while the complexity of our disease's genetics continues to present challenges, our network-based approach has successfully identified biologically plausible candidate genes and therapeutic opportunities deserving of further investigation.

References

[1] Thomas D. Bird. *Charcot-Marie-Tooth Hereditary Neuropathy Overview*. GeneReviews®[Internet]. University of Washington, Seattle, Seattle (WA), 2025. 1998 Sep 28 [Updated 2025 Jan 23].

[2] MedlinePlus Genetics. Charcot-marie-tooth disease, 2025. Cited: May 27, 2025.

[3] Natalie Vavlitou, Irene Sargiannidou, Kyriaki Markoullis, Kyriacos Kyriacou, Steven S. Scherer, and Kleopas A. Kleopa. Axonal pathology precedes demyelination in a mouse model of x-linked demyelinating/type i charcot-marie tooth neuropathy. *Journal of Neuropathology Experimental Neurology*, 69(9):945–958, 09 2010.

[4] Stephan Zuchner, Irina Mersiyanova, Maria Muglia, Nisrine Bissar-Tadmouri, Julie Rochelle, Elena Dadali, Mario Zappia, Eva Nelis, Alessandra Patitucci, Jan Senderek, Yesim Parman, Oleg Evgrafov, Peter Jonghe, Yuji Takahashi, Shoij Tsuji, Margaret Pericak-Vance, Aldo Quattrone, Esra Battaloglu, Alexander Polyakov, and Esra Battologlu. Mutations in the mitochondrial gtpase mitofusin 2 cause charcot-marie-tooth neuropathy type 2a. *Nature genetics*, 36:449–51, 06 2004.

[5] Brandon C. Farmer, Anna E. Walsh, Jack C. Kluemper, and Lance A. Johnson. Lipid droplets in neurodegenerative disorders. *Frontiers in Neuroscience*, 14:742, July 2020.

[6] Monica Valencia, Seong R. Kim, Youngeun Jang, and Seong H. Lee. Neuronal autophagy: Characteristic features and roles in neuronal pathophysiology. *Biomolecules Therapeutics*, 29(6):605–614, November 2021.

[7] Masamitsu Yamaguchi, Kentaro Omori, Satoshi Asada, and Hideki Yoshida. Epigenetic regulation of als and cmt: A lesson from drosophila models. *International Journal of Molecular Sciences*, 22:491, 01 2021.

[8] Guy Lenk, Cole Ferguson, Clement Chow, Natsuko Jin, Julie Jones, Adrienne Grant, Sergey Zolov, Jesse Winters, Roman Giger, James Dowling, Lois Weisman, and Miriam Meisler. Pathogenic mechanism of the fig4 mutation responsible for charcot-marie-tooth disease cmt4j. *PLoS genetics*, 7:e1002104, 06 2011. PMID:21655088.

[9] Shin Oh, Hyeongseop Kim, Sang eon Park, Jeong Kim, Yong Kim, Suk-Joo Choi, Soo-young Oh, Hong Bae Jeon, and Jong Wook Chang. Synergistic effect of wharton's jelly-derived mesenchymal stem cells and insulin on schwann cell proliferation in charcot-marie-tooth disease type 1a treatment. *Neurobiology of Disease*, 203:106725, 2024. PMID:39536952.

[10] Mohammadreza Emad, Hosein Arjmand, Hamid Farpour, and Bahareh Kardeh. Lipid-lowering drugs (statins) and peripheral neuropathy. *Electronic Physician*, 10:6527–6533, 03 2018.

Appendix

Gene	Degree	Betweenness	Eigenvector	Closeness	Betweenness/Degree
VCP	15	0.314644	0.405163	0.495575	0.020976
RAB7A	13	0.239473	0.364040	0.470588	0.018421
BAG3	10	0.106216	0.303257	0.427481	0.010622
LMNA	9	0.189731	0.168622	0.414815	0.021081
INF2	9	0.179926	0.257644	0.440945	0.019992
AIFM1	8	0.099257	0.196657	0.402878	0.012407
SLC25A46	8	0.164685	0.194008	0.414815	0.020586
DCTN1	7	0.061427	0.228121	0.368421	0.008775
HSPB1	7	0.083129	0.213608	0.414815	0.011876
DYNC1H1	6	0.037916	0.187785	0.388889	0.006319
GBF1	6	0.030166	0.256551	0.405797	0.005028
HK1	5	0.099855	0.134434	0.386207	0.019971
DCTN2	5	0.022859	0.128118	0.333333	0.004572
ATP1A1	5	0.012004	0.158428	0.378378	0.002401
NEFL	4	0.093442	0.034781	0.311111	0.023360
SBF1	4	0.050223	0.087281	0.337349	0.012556
ITPR3	4	0.028607	0.158786	0.383562	0.007152
ARHGEF10	4	0.027997	0.081562	0.347826	0.006999
HSPB8	4	0.039763	0.096871	0.337349	0.009941
SURF1	3	0.046374	0.015356	0.287179	0.015458
KIF1B	3	0.035714	0.057666	0.277228	0.011905
MME	3	0.009709	0.076275	0.335329	0.003236
JPH1	3	0.008723	0.113092	0.370861	0.002908
COA7	3	0.059210	0.060081	0.350000	0.019737
NDRG1	3	0.004351	0.101000	0.345679	0.001450
MTMR2	3	0.035714	0.023544	0.256881	0.011905
SLC12A6	3	0.012367	0.112076	0.341463	0.004122
DNM2	3	0.005338	0.147826	0.368421	0.001779
SBF2	3	0.022418	0.058161	0.320000	0.007473
HINT1	2	0.035714	0.065587	0.337349	0.017857
GNB4	2	0.035714	0.021762	0.282828	0.017857
ATP7A	2	0.035714	0.058929	0.325581	0.017857
PTRH2	2	0.004151	0.034094	0.311111	0.002076
SPTLC1	2	0.002695	0.056257	0.320000	0.001347
MFN2	2	0.000000	0.094576	0.350000	0.000000
SGPL1	2	0.002219	0.088502	0.347826	0.001109
SPG11	2	0.000000	0.098129	0.347826	0.000000
SIGMAR1	2	0.000866	0.042754	0.290155	0.000433
LRSAM1	1	0.000000	0.003716	0.205128	0.000000
CNTNAP1	1	0.000000	0.026616	0.294737	0.000000
LITAF	1	0.000000	0.047867	0.301075	0.000000
KIF5A	1	0.000000	0.026616	0.294737	0.000000
COX6A1	1	0.000000	0.002424	0.224000	0.000000
SETX	1	0.000000	0.040668	0.307692	0.000000
BSCL2	1	0.000000	0.030624	0.294737	0.000000
PLEKHG5	1	0.000000	0.003435	0.221344	0.000000
FIG4	1	0.000000	0.057461	0.321839	0.000000
PMP2	1	0.000000	0.010353	0.253394	0.000000
PDK3	1	0.000000	0.063953	0.333333	0.000000
FBLN5	1	0.000000	0.009102	0.217899	0.000000

Table 6: Main network metrics of disease LCC genes